environmental microbiology

Environmental Microbiology (2012) **14**(9), 2495–2510 doi:10.1111/j.1462-2920.2012.02767.x

Prokaryotic communities and operating metabolisms in the surface and the permafrost of Deception Island (Antarctica)

Yolanda Blanco,[1] Olga Prieto-Ballesteros,[2] Manuel J. Gómez,[1] Mercedes Moreno-Paz,[1] Miriam García-Villadangos,[1] José A. Rodríguez-Manfredi,[3] Patricia Cruz-Gil,[1] Mónica Sánchez-Román,[2] Luis A. Rivas[1] and Victor Parro[1]*

Departments of [1]Molecular Evolution, [2]Planetology and Habitability and [3]Instrumentation, Centro de Astrobiología (INTA-CSIC), Carretera de Ajalvir km 4, Torrejón de Ardoz, 28850 Madrid, Spain.

Summary

In this study we examined the microbial community composition and operating metabolisms on the surface and in the permafrost of Deception Island, (Antarctica) with an *on site* antibody microarray biosensor. Samples (down to a depth of 4.2 m) were analysed with LDChip300 (Life Detector Chip), an immunosensor containing more than 300 antibodies targeted to bacterial and archaeal antigens. The immunograms showed positive antigen-antibody reactions in all surface samples (lichens, pyroclasts) and the top layer of the permafrost. The results indicated the presence of exopolysaccharides, bacteria belonging to the *Alpha-*, *Delta-* and *Gammaproteobacteria*, *Bacteroidetes*, Gram-positive *Actinobacteria* and *Firmicutes*, as well as archaeal species, most probably *Methanobacterium* spp. Positive reactions with antibodies to proteins and peptides revealed the presence of nitrogen fixation (NifHD, GlnB, HscA), methanogenic (McrB), iron homeostasis and iron scavenging (ferritins and DPS proteins) proteins, as well as ABC transporters, which indicated that these processes were operating at the time of sampling. These results were validated with other molecular ecology techniques such as oligonucleotide microarrays, 16S bacterial rRNA gene sequence analysis, aerobic viable counts and microscopy. Molecular ecology results showed a differentiated pattern along the depth of the drill, being the top active layer the most diverse, with *Acidobacteria*, *Actinobacteria*, *Proteobacteria*, *Bacteroidetes* and the phototrophs *Cyanobacteria* and *Chloroflexi* as dominant groups. *Actinobacteria* and *Firmicutes* were dominant in depths from 0.5 to 2 m, and *Betaproteobacteria* from 3 to 4.2 m. The geochemical analysis revealed the presence of low molecular weight organic acids (acetate, formate) which could be used by microorganisms as energy sources for sulfate, nitrate and metal reduction under anaerobic conditions.

Received 18 November, 2011; accepted 9 April, 2012. *For correspondence. E-mail: parrogv@cab.inta-csic.es; Tel. +34 915201071; Fax: +34 915201074.

Introduction

It has been estimated that about 26% of terrestrial ecosystems correspond to permanently frozen soils, such as permafrost (Williams and Smith, 1989). Very often, the microorganisms living in these extremely cold habitats are true extremophiles in aspects, apart from their capacity to grow in the cold, such as their tolerance to high salt concentrations, oligotrophy or resistance to desiccation (due to low liquid water availability). Additionally, permafrost environments are considered terrestrial analogues for astrobiological studies because they can provide key information to evaluate the occurrence of life in other planetary environments like the permanently frozen martian soils (Gilichinsky *et al.*, 2007). Many studies have been conducted on permafrost, however, mostly on Arctic permafrost (reviewed in Steven *et al.*, 2006; 2009; Wagner, 2008), and only a few from the Antarctic (e.g. Gilichinsky *et al.*, 2007). Gilichinsky and colleagues (2007) reported the microbial diversity in old permafrost (5–8 Ma) obtained from drill cores in the Antarctic Dry Valleys. They found a diverse microbial population including aerobic and anaerobic prokaryotes (methanogens, sulfate reducers), cyanobacteria, green algae, yeasts and fungi. The diversity in the subsurface was similar to that of the active layer, suggesting this layer could act as the source of the microorganisms to the bottom layers.

For many years Deception Island (Antarctica) has been a natural laboratory for Vulcanologists, Geologists, Marine Biologists and Veterinarians, and several Nations have scientific stations to support research. However, very few geomicrobiological studies have been done there since

the studies of Stanley and Rose (1967) and Cameron and Benoit (1970). They investigated the culturable bacteria and yeast from several lakes of Deception Island, and reported that the Gram-negative rod-shaped bacteria predominated in all them, although one of the lakes contained large numbers of Gram-positive cocci and some others also contained yeast. Most of the microorganisms grew at temperatures below 20°C. Cameron and Benoit (1970) reported preliminary studies about the microbial ecology of recent cinder cones that arose in 1967 at Telefon Bay.

We focused on recent permafrost (approximately 200 years old) to get insights about how microbial populations colonize and establish themselves in the permanently frozen subsurface. We used an antibody microarray-based immunosensor developed in our laboratory, the LDChip300 (for Life Detector Chip), to monitor *on site* the microbial diversity and the presence of some metabolic indicators, such us enzymes involved in nitrogen fixation. LDChip300, initially designed for life detection in planetary exploration (Parro *et al*., 2005; 2008; 2011a), contains more than 300 antibodies developed against bacterial strains from almost all known phyla, crude extracts from environmental samples, biological polymers, proteins and peptides involved in selected metabolic pathways, cell wall components, etc. (Parro *et al*., 2008; 2011b,c; Rivas *et al*., 2008; 2011). By analysing the microbiology and the biomarker profiling associated to different depths and water content, our research may contribute the understanding of the ecology and the evolution of permanently frozen soils on Earth, from recent ones like this of Deception Island, to ancient ones like that of the Antarctica's Dry Valleys. In addition, permafrost grounds are good terrestrial analogues of the water ice-rich frozen grounds demonstrated at the Phoenix landing site on Mars (Smith *et al*., 2009). By studying the association of microbes to their mineral sources of energy from the volcanic material, our work may help to understand how a potential microbiota might have colonized, survived and evolved after past volcanism events on Mars. Finally, the low temperatures protect organic and biological matter from enzymatic activities and slow the kinetics of chemical degradation, which make the permafrost an ideal environment for biomarker detection and profiling.

Results

Geochemical analysis of the Deception Island permafrost

A 4.2 m deep drill was performed in a small plateau where the permafrost was composed of mineral volcanic deposits with a little to no visible soil layer (Fig. 1). The recovered cores showed high water content at the top part of the drill with large water ice crystals (Fig. 1C and D). The ice content and the size of the crystals diminished with depth, depending on the layer characteristics, until the cores were practically devoid of ice at 4.2 m. Samples from the cores (Table S1) were subjected to geochemical analysis to determine the main anions that could be used as carbon or energy sources for microbes. Significant amounts of Cl^-, SO_4^{-2}, NO_2^-, NO_3^-, PO_4^{-2}, and the low-molecular weight organic acids acetate, formate, propionate and oxalate were measured along the whole profile (Fig. 2). The acetate concentration showed peaks at the surface and at depths of 0.7 and 3.6 m, while formate, more irregular, showed a maximum at 3.6 m. Nitrate was only present from 0.6 to 2.5 m, while nitrite was only detected at 1 m with a concentration near 0.2 ppm. Sulfate was present along the whole drilling, with maximum from 0.9 to 2.5 m. Chloride showed relatively high concentrations between 0.9 to 3 m, with more than 60 ppm in several samples. These results revealed the presence of electron donors (e.g. formate and acetate) and electron acceptors (nitrates and sulfates) necessary for certain microbial metabolisms such us nitrate and sulfate reduction.

To have an estimation of the presence of biomolecules in the core samples, we determined total proteins and sugars extracted by ultrasonication (Fig. 2). Proteins showed two main peaks, one at the surface until a depth of 0.5 m, and a second one with a smooth slope from about 2.5 m to 4 m deep. The sugar pattern was more constant throughout the core with a small in increase at the bottom. This result indicated the presence of potential target biomolecules for immunological detection (see below).

On site detection of microbial markers in surface samples with LDChip300

Different samples (pyroclasts, fine clasts) on the surface around the drilling site (Fig. 1) were analysed by an *in situ* sandwich microarray immunoassay (SMI) with the LDChip300, a 300 antibody-containing microarray (Table S2) including antibodies to psychrophylic strains and representatives of the main phylogenentic groups of prokaryotes (Fig. S1). Up to eight samples and a blank control were simultaneously analysed per slide and, after scanning for fluorescence, an image was obtained from each sample (Fig. 3). The fluorescent signals were quantified and plotted to form an immunogram (Fig. 3). The most abundant and strongest positive signals were obtained with pyroclasts colonized by lichens, corresponding to antibodies raised against exopolymeric material from environmental extracts (water and sediments from an acidic environment), bacterial strains from the *Nitrospira* group, *Alphaproteobacteria* (*Acidiphilium*

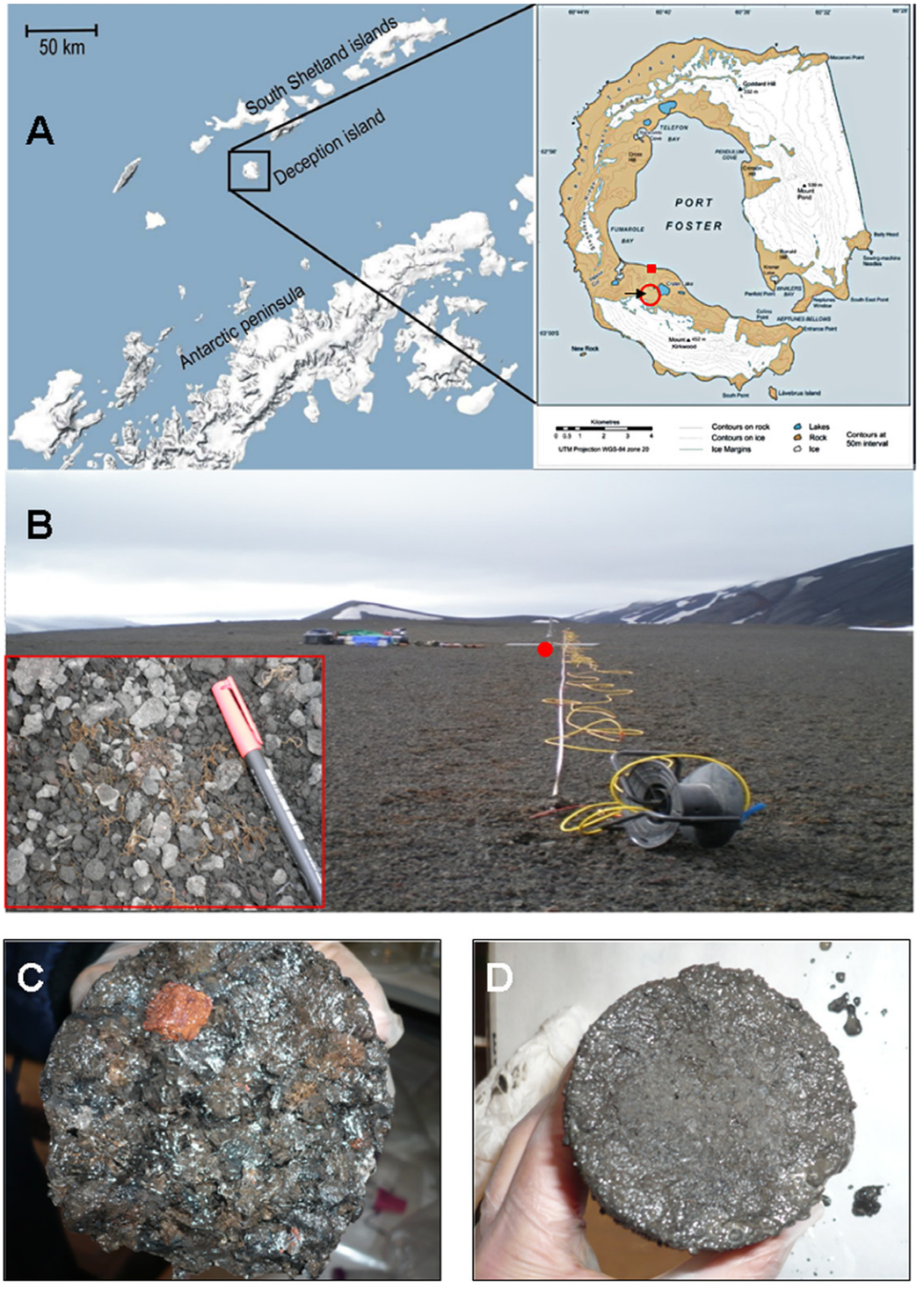

Fig. 1. Deception Island field site for permafrost drilling.
A. A map showing the northern of Antarctic Peninsula, the South Shetland Islands archipelago, and the Deception Island (insert), indicating the drilling site (red circle), close to the Spanish Gabriel de Castilla base (red spot).
B. A picture showing the plateau where drilling and sampling operations took place (red spot). The wires for the resistivity tests are shown. (Insert bottom left) a close up picture of a surface sample showing the fibers of decomposing moss between the pyroclasts.
C and D. Sectional views of cores obtained at depths of 60–80 cm, with high water content and big ice crystals (C), and from 2.7–2.8 m, with less water content and small ice crystals (D).

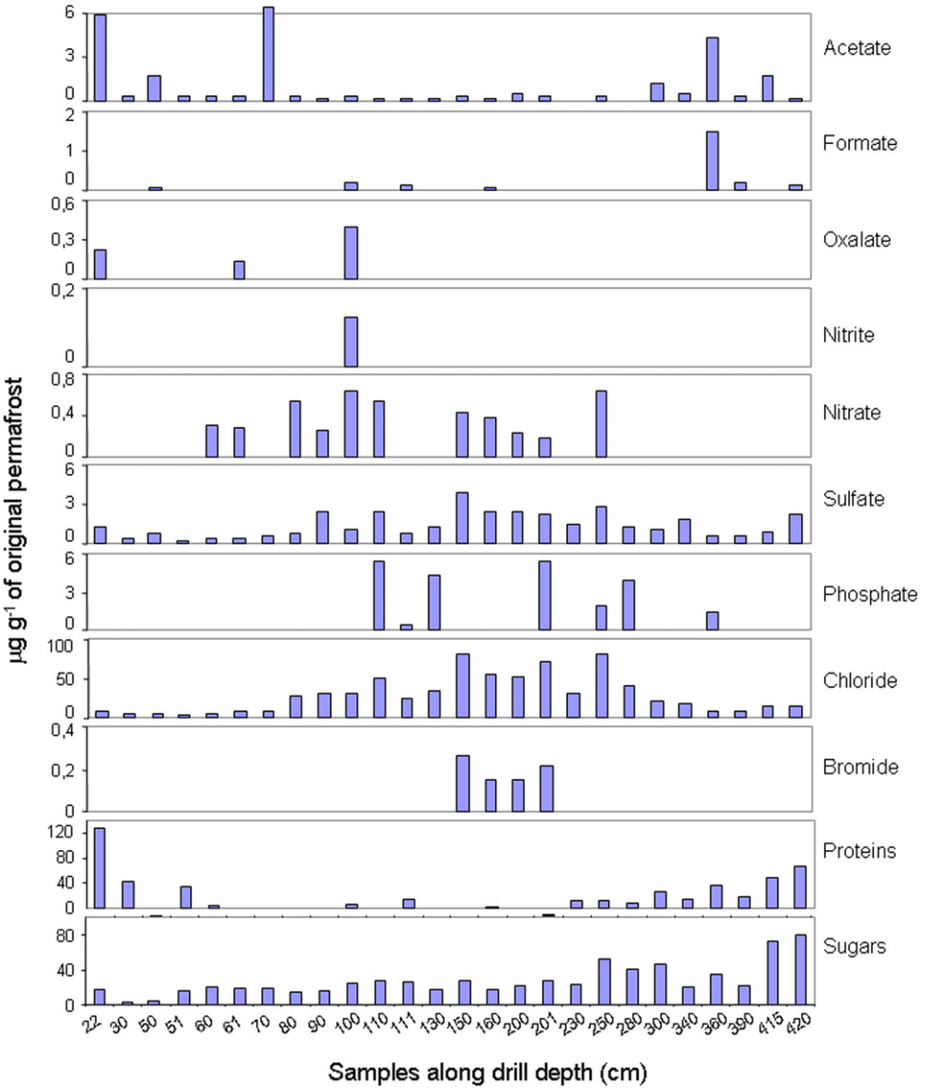

Fig. 2. Geochemical analysis of Deception Island permafrost. Distribution of low-molecular organic acids and main inorganic anions with depth. Anions were dissolved from permafrost samples as indicated in Experimental procedures and determined by ion chromatography. Also (last two bottom charts) determination of total proteins and sugars content in the samples analysed with LDChip300 (see below).

spp.), *Gammaproteobacteria* (*Acidithiobacillus* spp., *Pseudomonas* spp. or *Azotobacter* spp.), *Acidimicrobium* spp., *Acidobacterium* sp., *Firmicutes* (*Desulfosporosinus* spp. and *Bacillus* spp.), antibodies against exopolysaccharides (EPS), and against proteins and peptides related to nitrogen fixation (ferredoxins, iron-sulfur cluster formation chaperon HscA, and nitrogenase components NifH, NifD, NifS), and methanogenesis (McrB, the beta subunit of methyl coenzyme-M reductase I). Additionally, positive signals were also detected with antibodies to archaeal strains such as *Methanobacterium* spp. and *Halorubrum* spp. (Fig. 3 and Table S3). Positive immunological reactions were obtained from some pyroclasts without any visible signs of life (sample DCS6; Fig. 3), but lichen-containing samples showed the strongest immunoreactive signals and the most diverse immunograms (see sample DCS7, Fig. 3), with clear reactions against proteins related to nitrogen fixation and EPS (peaks 15, 56 and 57. Table S3).

Microbial biomarker profiling of the Deception Island permafrost with LDChip300

Core samples from intact permafrost were also analysed by SMI with LDChip300. The immunograms showed several positive antigen–antibody reactions mainly in the upper samples, near the surface deposit and the surface pyroclast (Fig. 4). Most of the positive spots

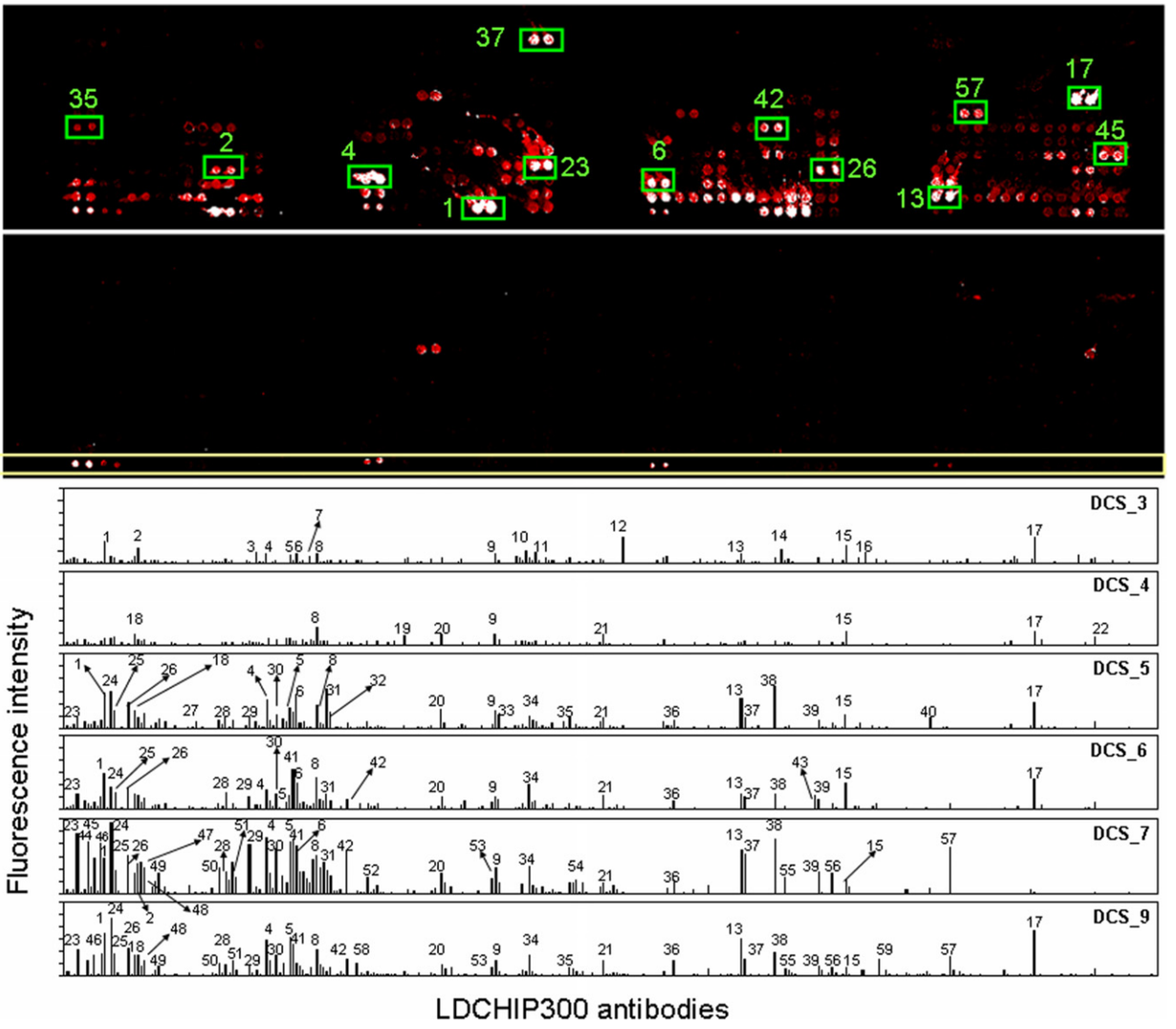

Fig. 3. The LDChip300 detected microbes and biological polymers in surface pyroclasts. A representative scanned image of LDChip300 obtained after the analysis of a lichen-containing rock by sandwich microarray immunoassay (top panel) and the negative control image showing only the positive control spots (bottom panel). Fluorescent intensity ranges from 0 (black) to 65.000 relative units (white). The fluorescence intensity obtained after the analysis of different surface samples (DCS3-DCS9) was quantified and plotted (bar diagrams or immunograms). The numbers indicate the antibodies showing positive reactions (Table S3), among them the antibodies to: *Acidimicrobium ferrooxidans* (42), *Acidiphillium* sp. (20), *Shewanella gelidimarina* (52), *Desulfosporosinus meridiei* (53), *Pseudomonas putida* (9), *Bacillus* sp. (34), *Acidithiobacillus* spp. (5, 6, 31), etc.

corresponded to cellular and EPS environmental extracts (water, sediments, filamentous biofilms, deep cores, iron-sulfur precipitates) from Río Tinto (Spain) enriched in *Gammaproteobacteria* (genus *Acidithiobacillus*) and *Leptospirillum* spp., psychrophiles such as *Colwellia psychrerythraea* and *Shewanella gelidimarina*, *Pseudomonadacea*, Gram-positive *Firmicutes* (*Bacillus* spp. and *Desulfosporosinus* spp.), *Deltaproteobacteria* (*Desulfotalea psychrophila*), other psychrophiles from the *Bacteroidetes* and *Actinobacteria* groups, and some archaea, including a methanogen (Table 1). Most of these positive reactions were previously detected in the surface samples (see above), but others seemed to be specific of the first centimetres of active permafrost, such as *D. psychrophila* (facultative anaerobe heterotroph), *S. gelidimarina* (anaerobic, iron, manganese, and nitrate reducer), *Cryobacterium psychrophilum* and *C. psychrerythraea* (Table 2). Additionally, significant fluorescent signals were obtained with antibodies against peptides and proteins related to relevant metabolic pathways: iron metabolism (reduction, capture and homeostasis), nitrogen fixation, active transport mediated by ABC

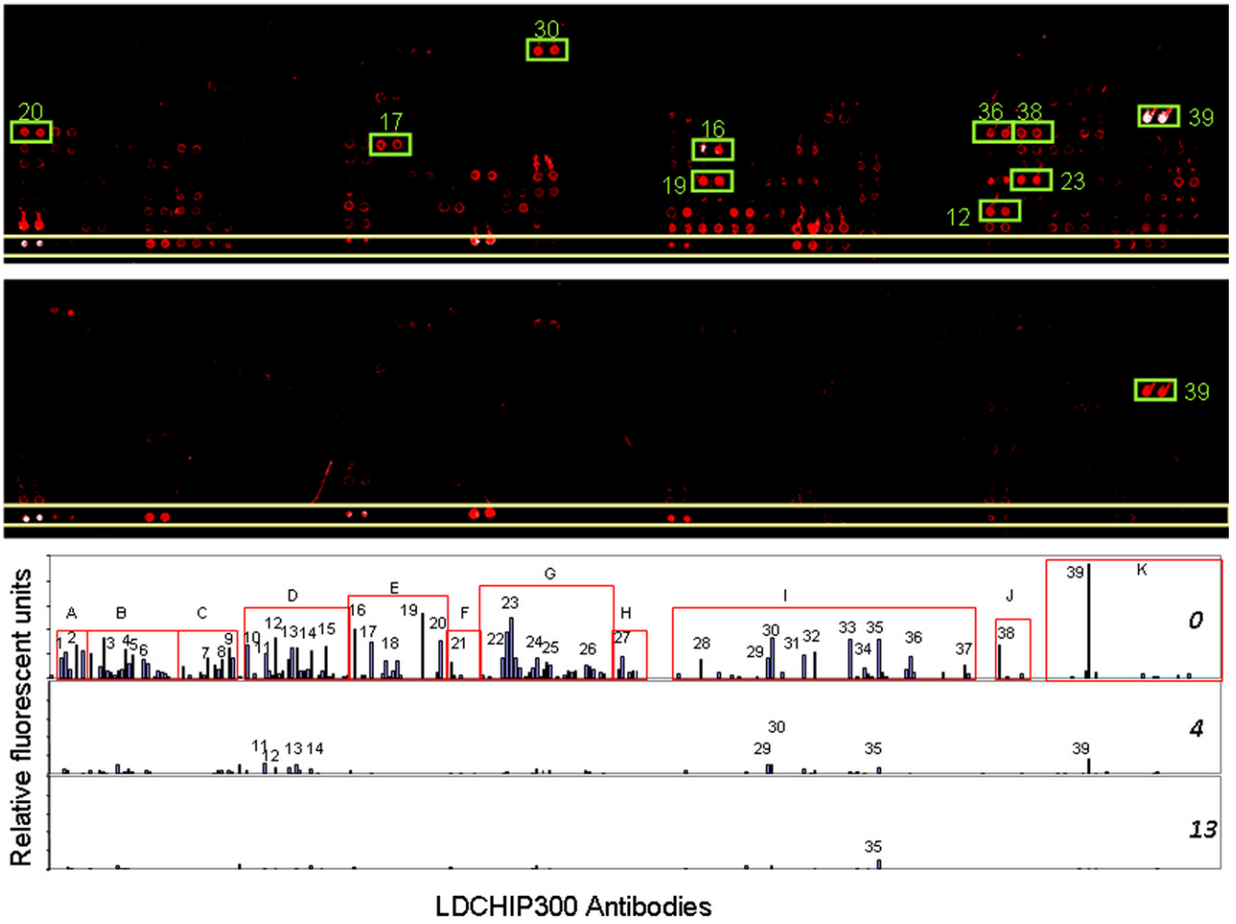

Fig. 4. The LDChip300 detected microbes and biological polymers in the top active layer of the Deception Island permafrost. A representative scanned image of LDChip300 obtained after the analysis of a subsample from the top active layer (sample ***0***, from 0 to −4 cm) by sandwich microarray immunoassay (top panel) and the negative control image (bottom panel). The fluorescence obtained with the different samples was quantified and plotted (immunograms). The numbers over the peaks indicate the most relevant positive reactions (see Table 1), some of them highlighted on the scanned image (top). Numbers to the right of the immunograms indicate the sample ID: ***0*** (active top layer from 0 to −4 cm), ***4*** (4 to −13 cm) and ***13*** (13 to −22 cm).

transporters and Fe-S cluster formation (Table 1). Also, anti-EPS antibodies showed a strong signal, revealing the presence of abundant EPS in the samples. The immunological reactions obtained with the LDChip300 decreased sharply after 5 cm in the active permafrost (Fig. 4). Only after the analysis of concentrated crude extracts (see *Geochemical analysis*) positive immunoreactions were detected (Fig. S2) corresponding, mainly, to sulfur oxidizing *Betaproteobacteria* from the genus *Acidithiobacillus*.

Microscopic analysis and viable cells counts

Several permafrost core samples were also analysed by optical and scanning electron microscopy (SEM) (Fig. 5). Unspecific DNA staining with DAPI showed various cell morphologies, including chains of rods and cocci cells and microcolonies either free or bound to minerals along the whole drilling (Fig. 5A). Fluorescent *in situ* hybridization (FISH) staining with a universal probe for bacteria distinguished metabolically active cells from others that might of been dead, inert (spores) or archaea, which are not targeted by the probe (Fig. 5A and B). In fact, a cluster of living bacterial and archaeal cells was detected in a 0.7–0.8 m deep core sample by dual staining with bacterial and archaeal FISH probes (Fig. 5C). The SEM images also showed several microbial morphologies and polymeric substances bound to mineral surfaces (Fig. 5D and E), even at a depth of 3.5 m (Fig. 5F).

Viable aerobic cells were estimated along the whole drilling by culturing in a rich medium at 20°C (Table S4). These conditions were used as a compromise to obtain the higher numbers of colonies, without using multiple culturing conditions. This approach was supported by the

Table 1. List of the antibodies that showed positive reactions after analysing the top active layer with the LDChip300, and a comparison of that data to PAM (prokaryotic acidophile microarray) and 16S rRNA gene sequencing (Seq) results.

	LDChip300					
Peak	Ab name	Immunogen	Antigen type	Phylogeny	PAM	Seq
21	IVG2C1	*Acidiphillium* sp. (*Acetobacteraceae*)		*Alpha*	+	+
1	IA1S1, S2	Río Tinto (3.2 water dam)	EPS from acidic waters	*Gamma*	+	+
2	IA2S1, IA3S1	Filamentous biofilm (EPS)				
3	IC1C1, IC2C3	Sediments Playa (cells)	Cells and EPS from sediments			
4, 5	IC3C1, C3, S2	Brown filaments (cells)	and salt precipitates			
6	IC5C1, IC5S1	Red iron crusts				
7	ID1C1, S1, S2	Iron-ulfate rich precipitates (cells)	Cells and EPS			
13	IVE3C1, C2, S1	*Acidithiobacillus ferrooxidans*	Cells and EPS			
14	IVE4C1, C2	*Acidithiobacillus thiooxidans*				
15	IVE5S100	*Acidithiobacillus albertensis*				
17	IVF2S2	*Shewanella gelidimarina* EPS 4°C	EPS from psychrophiles			
20	IVF7S2	*Colwellia psychrerythraea* EPS				
22, 23	IVI1C1, C2	*Pseudomonas putida* (cells)	Cells and proteins			
24	IVI3C1	*Shewanella oneidensis* (cells)	Aerobic			
26	IVI5S1, S100	*Shewanella oneidensis* (EPS and S100 proteins)	Anaerobic			
16	IVF18C1	*Desulfotalea psychrophila*	Cells	*Delta*	+	+
10, 12	IVE0C_139, IVE2S1	*Leptospirillum* spp.	Cells, EPS	*Nitrospira*	+	ND
19	IVF6S1	*Cryobacterium psychrophilum*	EPS, psychrophiles	*Actinobacteria*	+	+
24	IVI2C1, S2	*Bacillus* spp.	EPS and cells	*Firmicutes*	ND*	ND*
22	IVI19C1	*Desulfosporosinus meridiei*	Cells		ND*	ND*
18	IVF4S1, S2	*Psychroserpens burtonensis*	EPS	*Bacteroidetes*	ND	+
27	IVJ4C1	*Methanobacterium formicicum*	Cells	Archaea	?	?
8,9	ID2S2, ID4S2	148, 154, 141 m Pyrite-rich deep cores	EPS subsurface		?	?
28	Prot_ABC transporter	Mo transport for nitrogenase	Peptides	ABC transporters		
33	Prot_ModA2_1494					
30	Prot_FeReTs_983	Iron reduction. *S. gelidimarina*	Protein	Oxido-reduction		
29	Prot_Fdx2_1490	Fe-S cluster formation. Electron chain	Peptide			
31	Prot_HscA2_1487	Fe-S cluster formation chaperone	Peptides	N2 fixation		
34	Prot_NifD2_1485	Nitrogen fixing bacteria				
35	Prot_NifH3_1484					
32	Prot_HuFER	Iron storage protein: iron limitation	Purified proteins	Iron homeostasis		
36	Prot_PfuFER	and/or detoxification				
37	Prot_SsoDPS					
38	vvCW_EPS_SP	EPS	Purified EPS	Solar saltern		
39	wwsm_dinitrophenol			Xenobiotics		

+, positive reaction with probes on the PAM microarray or positive detection of 16S rRNA gene sequences from a member of the phylum or group. ND, not detected. ?, not tested. ND*, not detected in this sample but positive in others (see Figs S4 and S6). Peak, peak numbers from Fig. 4.
Alpha-, Gamma- and *Deltaproteobacteria*.
Shade and white spaces are used to separate different groups of antibodies for easier reading.

Table 2. Main differences in the positive antibody reactions between surface samples and the permafrost active top layer obtained with LDChip300.

Surface (pyroclasts) samples		Active layer permafrost	
Ab name	Antigen description	Ab name	Antigen description
138	EPS from Rio Tinto (RT) sediments	IC5C1, S1	Cell/EPS from red iron crusts (RT)
IC4C1	Cell extract from brown filaments (RT)	ID13S2	EPS from 2 m deep core sample (RT)
IC6C1	Cell extract red sediments (RT)	IVF7S2	EPS from *Colwellia psychrerythraea*
ID15S2	EPS from 119 m deep cores (RT)	IVI1RB, S100	Ribosomes and S100 extracts *Pseudomonas putida*
IVE1BF, S1	*Leptospirillum pherrifilum* (LPH2) from fermenter	IVF18C1	Cell from *Desulfotalea psychrophila*
IVE5C1, C2	*Acidithiobacillus albertensis*	IVF6S1	EPS from *Cryobacterium psychrophilum*
IVE6C1, C2	*Acidithiobacillus caldus*	IVI21S1	EPS from *Salinibacter ruber*
IVE8S2	*Acidimicrobium ferrooxidans*	IVF4S1, S2	EPS from *Psychroserpens burtonensis*
IVF2C1	*Shewanella gelidimarina* Cells 4°C	IVJ3C1	Cells from *Thermoplasma acidophilum*
IVF5S100	*Psychrobacter frigidicola* S100 extract	IVJ9C1	Cells from *Halobacterium* sp.
GlnB2_1492	Global Nitrogen regulator GlnB	ID5S2_254	EPS from a 141 deep core (RT)
McrB	Methyl CoM reductase I, B subunit	Prot_PfuFER	Ferritin from *Pyrococcus furiosus*
HtpG	Cold adaptation in *Cyanobacteria*	Prot_PfuDPS	DPS protein from *Pyrococcus furiosus*
OmpA	OmpA membrane protein	Prot_SsoDPS	DPS protein
PhA_1	Iron scavenging regulator		
Stv	Streptavidin (*Actinobacteria*)		

Each column shows the list of antibody-antigen pairs which showed a positive reaction exclusively the respective sample.

presence of decomposing organic matter from the surface mosses and lichens in the surface, which suggested that a rich medium would be appropriate. Also, because this terrain came from a relatively recent volcanic eruption, resistant forms of mesophiles or moderate thermophiles might still be recovered by incubating at 20°C. The viable cells count showed an irregular distribution but a clear maximum near the surface (10^3–10^4 cfu g^{-1}), and other peaks at depths around 2–2.3 and 3–3.4 m. The colonies showed diverse morphologies and pigmentations (Fig. S3). Microscopic analysis after DAPI staining revealed the presence of bacilli, cocci and filamentous bacteria (most likely actinobacteria) (Fig. S3). The 16S rRNA gene sequence analysis of some colonies identified bacteria belonging to the genera *Arthrobacter*, *Polaromonas*, *Rhodococcus*, *Sporosarcina*, *Kocuria* and *Subtercola*, all of them previously detected in other Arctic or Antarctic environments (Table S5).

Molecular ecology of Deception Island permafrost

The results obtained with LDChip300 were partially corroborated *on site* by DNA extraction, polymerase chain reaction (PCR) amplification of 16S and 23S rRNA genes, fluorescent labelling and hybridization with an oligonucleotide microarray for prokaryotic diversity (*Experimental procedures*). DNA probes revealed the presence of *Alpha*- and *Deltaproteobacteria*, and high GC-content Gram-positive bacteria (*Actinobacteria*) in sample from the top active layer (Fig. S4, Table 1). Gram-positive *Firmicutes* showed and irregular pattern, appearing at 0.7, 3.0 and 4.15 m deep but absent in samples taken from other depths, while *Betaproteobacteria* clearly dominated in the deepest samples.

Additionally, DNA from core subsamples was used for amplification, cloning and sequencing of the 16S rRNA gene. The phylogenetic analysis (Figs S5 and S6) was consistent with the immunological results obtained with LDChip300 in the active top layer, in that the microbial community was dominated by *Alpha*-, *Beta*-, *Delta*- and *Gammaproteobacteria*, *Actinobacteria* (high GC-content), *Bacteroidetes*, and the nitrogen fixing *Cyanobacteria*, which may account (among other nitrogen fixing bacteria) for the positive signals with antinitrogenase protein components antibodies (Fig. 6, Table 1). Additional sequences were identified as members of the *Acidobacteria* and *Verrucomicrobia* groups.

Representatives of almost all bacterial phyla were detected along the entire drilling, with a specific distribution as a function of depth (Fig. 6). The top layer contained a high level of prokaryotic diversity, as indicated by a Simpson index value of 0.018, with representatives of several bacterial phyla. It was mainly dominated by *Actinobacteria*, *Cyanobacteria* (*Nostoc* spp.), *Acidobacteria* and *Proteobacteria* (*Alpha* > *Beta* > *Gamma* > *Delta* subdivisions). The rarefaction curves (Fig. S5) indicated that the current sequencing effort had captured only a fraction of the microbial diversity of this level of the active permafrost. Below approximately 0.5 m and down to 1 m, about 40% of operational taxonomic units (OTUs) were classified as low GC-content Gram-positives *Firmicutes* (all *Clostridia*), which had not been detected in the top layer. Also, *Actinobacteria* and *Proteobacteria* (*Alpha* > *Gamma* > *Beta*) were abundant, while photosynthetic *Cyanobacteria* were completely absent. From 1 to 2 m of depth, 40% of the OTUs were classified as *Actinobacteria* (half of them *Actinomycetales* and half unclassified), followed by 25% of *Proteobacteria* (*Gamma* > *Beta* >

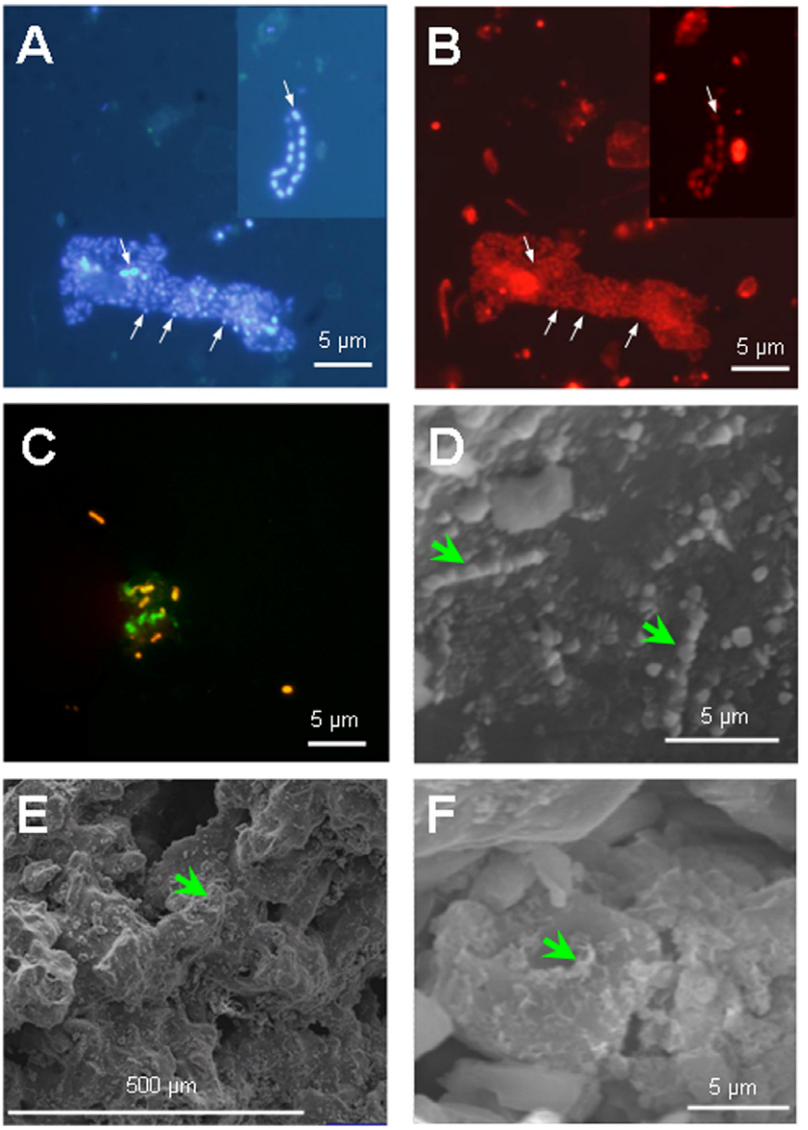

Fig. 5. Optical and SEM microscopy of permafrost samples.
A and B. DAPI (A) and FISH stain with an eubacterial probe (B) showed chains and clusters or microcolonies of cells in a sample from the top active layer (sample ***0***). The arrows indicate the cells stained with DAPI but not with the FISH probe (see text for explanation).
C. A cluster of bacterial (orange) and archaeal (green) cells as detected with specific FISH probes in a sample from a depth of 70–80 cm.
D–F. SEM images showing single and chains of microbial cells attached to the mineral surface in sample ***0*** (D), and showing extracellular polymeric substances in samples ***0*** (E) and ***415*** (–4.15 m) (F).

Alpha), 25% of unclassified, and few representatives of the remaining phyla. From 2 to 2.5 m the presence of *Actinobacteria* diminished while that of *Proteobacteria* increased. From 2.5 to 3.0 m there was a sharp change in the pattern, which became mainly composed by *Proteobacteria* (most of them *Beta*-) and *Firmicutes*. Finally, from 3 to 4 m the pattern was dominated by *Proteobacteria* (> 80% of the sequences; *Beta* >> *Alpha* = *Gamma*), and some representatives (less than 20% to 5% of the sequences) of the other phyla, being *Gemmatimonadetes* and *Firmicutes* the most abundant among them. The change in bacterial community membership observed as depth increased was associated to a reduction in microbial diversity, having the last level an associated Simpson index value of 0.219. A phylogenetic tree illustrating the overall bacterial diversity is shown in Fig. S6.

Discussion

Immunoprofiling the microbial community of Deception Island

In this work we demonstrate the potentiality of LDChip300 technology to profile the diversity of natural microbial communities and to determine their main operating metabolic pathways. The relatively strong immunoreactions with rock samples without any visible sign of life (samples DCS3, 5 and 6 in Fig. 3) supported that our LDChip is a powerful tool for life detection and biomarker profiling and suggested that endolithic microbes are contributing to supply abundant immunoreactive polymeric or cellular material in Deception Island's permafrost. Positive reactions with antipeptide and antiprotein antibodies related to iron homeostasis and metabolism, nitrogen fixation, iron-sulfur cluster

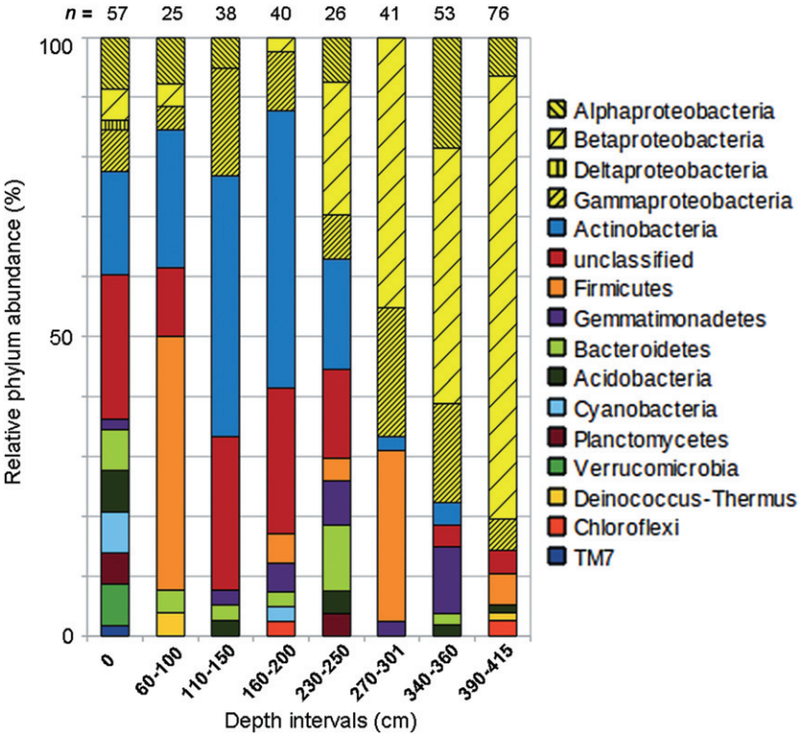

Fig. 6. Phylogenetic distribution and frequencies of the clones obtained from total community 16S rRNA gene cloning and sequencing of Deception Island permafrost. Samples were clustered at different depth intervals (cm). The total number (*n*) of the clones included in the analysis is indicated (top).

formation, active ABC transport, together with other positives with antibacterial strains and EPS, provided clues regarding the metabolic pathways that may be operative in Deception Island's permafrost: nitrogen fixation, iron and sugar metabolisms, or EPS formation. Positive reactions with antibodies to ferritins and DPS proteins indicated a relevant metabolic activity for iron scavenging or detoxification (Andrews *et al*., 2003).

Surface samples showed immunoreactions with antibodies against acidophilic microorganisms and biofilms (Fig. 3 and Table S3) suggesting acidic microniches on the surface of the pyroclasts. The positive reactions with anti-McrB and anti-*Methanobacterium formicium* indicated the presence of methanogens in some of the samples, probably in the deepest parts of biofilms or internal parts of the pyroclasts.

Positive immunoreactions with antibodies to psychrophiles *D. psychrophila*, *Cr. psychrophilum*, *Psychroserpens burtonensis*, *C. psychrerythraea* and *S. gelidimarina* in the active top layer (Fig. 4) revealed the presence of these psychrophilic bacteria or very close relatives in the active layer. *C. psychrerythraea* is considered a facultative anaerobe with important adaptations for survival in cold environments like the production of extracellular polysaccharides for the protection against cold-damage (cryoprotection) (Marx *et al*., 2009). This may be one of the reasons why LDChip300 showed many positive reactions with antibodies to EPS (Table 1). Species of the genus *Shewanella* are facultative anaerobic chemoheterotrophs able to grow anaerobically by fermentation on N-acetylglucosamine and chitin or by reducing nitrate and ferric compounds by using low-molecular organic acids like acetate as electron donors (Bowman *et al*., 1997b). The positive immunoreactions obtained with antibodies to an outer membrane iron reductase (anti-FeReTs) and a ferredoxin peptide (anti-Fdx) in LDChip300 suggested that iron or other metal reduction pathways were operating in the active layer. The presence of *Shewanella* spp. and other metal reducing strains together with fact that sugars and organic acids were indeed detected (Fig. 2) support this idea. A strong signal was also obtained in the anti-*D. psychrophila* antibody spot, a marine sulfate-reducing delta-proteobacterium able to grow at temperatures below 0°C (Rabus *et al*., 2004). *Desulfotalea* spp. uses the most common fermentation products in marine sediments, such as acetate, propionate, butyrate, lactate and hydrogen as electron donors and sulfite and thiosulfate as electron acceptors (Knoblauch *et al*., 1999). The *Actinobacterium Cr. psychrophilum*, also detected in the active top layer, is an obligatory psychrophile originally isolated from Antarctica and capable of producing acid from several monosaccharides (Suzuki *et al*., 1997). Another Antarctic bacterium, *P. burtonensis* (*Bacteroidetes*) was detected in the active layer and may be metabolizing the acids produced by other bacteria with fermentative metabolisms of sugars, EPS or other

complex polymers from decomposing moss from the near surface (Bowman *et al*., 1997a).

The lack of immunoreactions below the top active layer (Fig. 4) may be due to a sharp drop in the number of microorganisms and EPS to levels that are below the limit of detection of our system, or to a shift in microbial diversity that is not covered by the collection of antibodies currently included in LDChip300. The results indicated that it might be a consequence of both factors: first, viable cell counts dropped as depth increased; second, while 16S rRNA gene sequence surveys indicated that *Betaproteobacteria* dominated in the deepest samples, the presence of this phylum was only detected with the anti-*Burkholderia fungorum* antibody in our microarray (Fig. S1, Table S2).

Bacterial diversity in the permafrost of Deception Island

Microscopic analysis showed very diverse microbial morphologies, such as chains and clusters. FISH staining revealed the presence of bacterial and archaeal clusters which might constitute metabolically active consortia (Fig. 5C). Most of the 16S rRNA gene sequences we obtained were similar to other sequences in the GeneBank database that had been recovered from Arctic, Antarctic, glacial or ice environments. The molecular phylogenetic analysis corroborated and expanded the results obtained with the LDChip antibody microarray (Table 1). Furthermore, it provided an overall picture of the microbial diversity along the permafrost column, which included carbon and nitrogen fixers and photosynthetic bacteria, together with heterotrophs in the top active layer, *Firmicutes* in the middle segment, and metal reducing *Betaproteobacteria* at the deepest portion (3–4 m) of the drill (Fig. 6).

The Gram-positive high GC-content *Actinobacteria* dominate down to 2 m deep, as it was reported in a Canadian Arctic permafrost (Yergeau *et al*., 2010), with a major presence of the *Rhodococcus* spp. with many unclassified OTUs at the bottom, while *Pseudonocardia* spp. and others were in the active layer. Low GC-content Gram-positive *Firmicutes* were not detected in the few centimetres of the top active layer but were especially abundant at depths between 0.7 to 1 m, most of them being classified within the order *Clostridiales* which, together with other unclassified OTUs, showed 93–94% sequence identity to bacterial clones obtained from cultures enriched in nitrate reducers and denitrifiers (Ishii *et al*., 2009). In addition, a peak of acetate was measured between 0.7 and 0.8 m deep (Fig. 2), suggesting the possibility of acetic acid producing *Firmicutes* in the permafrost.

Two clones were classified as belonging to the phylum *Deinococcus*/*Thermus*. One of them close to *Meiothermus silvanus*, isolated from hot spring and whose optimal growth temperature ranges from 40°C to 60°C (Sikorski *et al*., 2010). The presence of this type of bacteria was in agreement with the hydrothermal and volcanic history of the geological substrate that makes the Deception Island permafrost. The other clone was similar to *Deinococcus marmoris*, a Gram-positive, non-motile, UV- and draught-tolerant bacterium isolated from an Antarctic marble sample (Hirsch *et al*., 2004).

The *Proteobacteria* were present throughout whole drilling; however the distribution of the various phyla varied. *Alpha-*, *Beta-* and *Gammaproteobacteria* were present throughout the drill while *Deltaproteobacteria* were only found in the active top layer. Additionally *Betaproteobacteria* were the dominant proteobacteria from a depth of 3 m to the bottom. Within *Beta-*, the genus *Polaromonas* was abundant at 3–4 m, while there was a sharp increase in the numbers of sequences classified as *Ralstonia* spp. below 3.5 m. Up to 20 clones showed 97% identity to *Polaromonas hydrogenivorans*, a psychrotolerant (0–25°C), chemolithotrophic Gram-negative cocci isolated from Alaskan forest soil capable of growing autotrophically on H_2/CO_2 mixtures and to switch to heterotrophic growth on organic substrates (Sizova and Panikov, 2007). The highest identity (99.4–99.9%) within *Ralstonia* spp. (54 sequences) corresponded to iron (III)-reducing enrichment sequences in sediments of the polluted Scheldt estuary, Northwest Europe (Lin *et al*., 2007) and soil polluted with heavy metals (GeneBank no. GQ487980.1). Therefore, our data supported the presence of metal-reducing anaerobe facultative bacteria in the Deception Island permafrost.

Clones showing the best similarities to iron oxidizing bacteria were also identified in the samples taken at depths of 1.5–1.6 (most of the clones), 2.0 and 2.6 m. Some of them (seven clones) showed 96–97% identity with environmental clones obtained from drainage waters of uranium waste piles (Selenska-Pobell, 2002) and 90.77% to *Acidiferrobacter thiooxydans*, and acidophilic, thermo-tolerant, facultative anaerobic iron- and sulfur-oxidizer very similar (99%) to *Acidithiobacillus ferrooxidans* strain DSM 2392 (Hallberg *et al*., 2011). Another clone was obtained at 3.0 m deep with 98.3% sequence identity to a sulfur-oxidizing bacterium isolated from perennially ice-covered Lake Fryxell, in Dry Valleys, Antarctica (Sattley and Madigan, 2006). This result was in agreement with the positive reactions obtained with anti-*Acidithiobacillus* spp. antibodies when crude extracts were assayed with LDChip300 (Fig. S2). The presence of *Acidithiobacillus* spp. or other iron and sulfur oxidizing acidophile bacteria might be associated to acidic microniches, probably due to sulfur and/or iron containing minerals like Maghemite (Fe_2O_3, γ-Fe_2O_3), found at depths of around 1 m (O. Prieto-Ballesteros, pers. comm.). In fact,

Cameron and Benoit (1970) reported layers of acidic (around pH 3) volcanic material formed within 1 year after the eruptions. This acidic material might have been good substrate for the development of acidophiles, and subsequent burial of those layers would have been trapped in the permafrost.

Conclusions

The Deception Island mineral permafrost showed a clear humidity gradient, from high ice content in the upper parts to almost desiccated at a depth of 4.2 m, indicating that water supply came from the meteorological water after snow melting. The LDChip300 results together with 16S rRNA phylogeny confirmed a diverse microbial community colonizing the surface of the permafrost. Strong immunoreactions indicative of specific metabolisms (nitrogen fixation, iron reduction and homeostasis, methanogenesis, or nutrient transporters) were consistent with the molecular phylogenetic analysis, which confirmed the presence of bacterial strains capable of performing these metabolic functions (Figs 6 and 7). The microbial community showed a well-stratified distribution, with a gradual increase in *Betaproteobacteria* from 2 to 4.2 m of depth. Deception Island permafrost seemed to be dominated by facultative anaerobes with high capacity of metal (mainly iron) and nitrate reduction. The electron sources for these processes could come from the organic matter synthesized by the primary producers on the surface (*Cyanobacteria*, *Chloroflexi*, lichens, moss) and then hydrolysed and fermented by *Actinobacteria*, *Acidobacteria*, *Bacteroidetes*, *Planctomycetes* and others. The geochemical results supported the anaerobic operating metabolisms, where low-molecular organic acids (acetate, formate) can be used as energy and/or carbon sources for metal (e.g. Fe^{3+}), nitrate, and sulfate reduction.

Experimental procedures

Field site, resistivity tomography, drilling and sampling

Deception Island is an active volcanic island where recent eruptions have been reported. The most recent one occurred in 1967–1970, in the north coast of the Port Foster (Baker and McReath, 1971). The main objective of our research was to study the microbial diversity of the very young permafrost located in a small plateau composed of volcanic material from a recent volcanic eruption (c.a. 200 years ago). The surface contains coarse material mainly made up of basaltic pyroclasts of different sizes, but not larger than 2–4 cm, with brown fibres of decomposing moss between them. The permafrost of the area around the drill hole was studied using the electric resistivity tomography technique by means of a Syscal Kid switch 24 equipment. Electric resistivity tomography profiles were taken with lengths ranging from 23 to 47 m, with electrodes spaced between 1 to 2 m and a maximum penetration depth of 5 m. Resistivity tests and the manual check by means of an iron bar indicated that the permafrost was between 20 and 30 cm below the surface.

A small plateau (coordinates: 62°59′10.22″S, 60°40′32.36″W) to the South of the Spanish base 'Gabriel de Castilla' was chosen for sampling and drilling operations. The drilling was done with a gas-powered machine CARDI EN 400 with a maximal power of 4.08 HP (horse power); with an

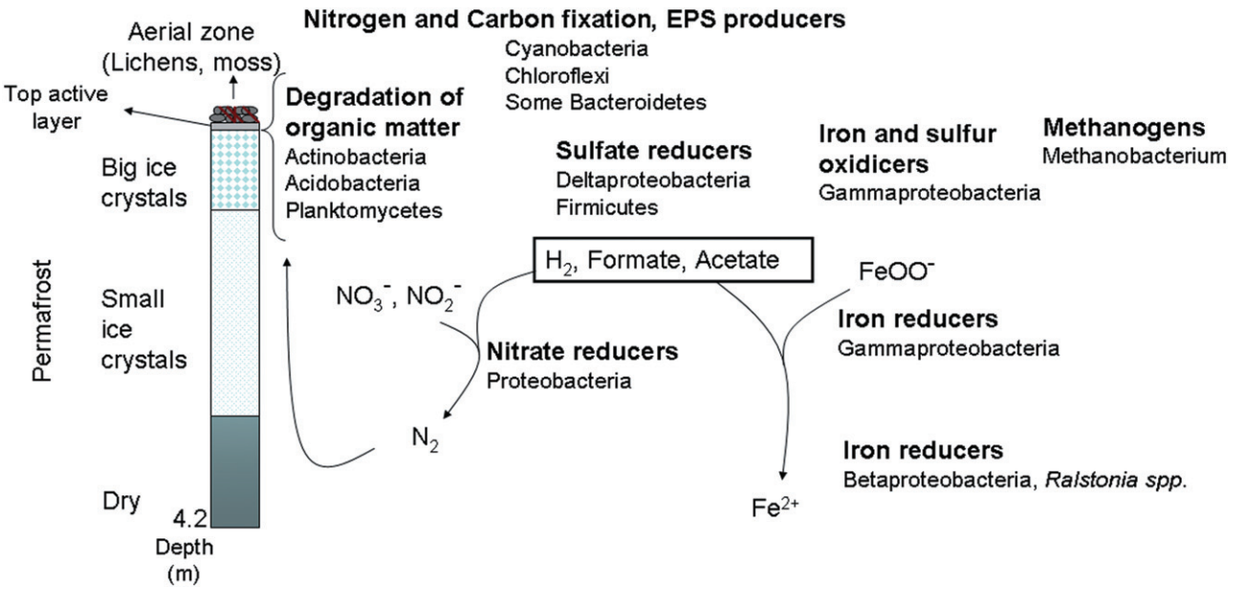

Fig. 7. A scheme showing the main prokaryotic Phyla and the operating metabolisms identified in the Deception Island surface and permafrost (see text for explanations).

85 mm diameter COTS (Commercial Off-The-Shelf) impregnated diamond core drill bits and rods as described in Parro and colleagues (2011b). See also Supporting Information for details. Core samples of permafrost were obtained along the whole drilling at different depths (Table S1).

Geochemical analysis

Ion chromatography was used to measure the main anions (Cl^-, SO_4^{-2}, NO_2^-, NO_3^-, PO_4^{-2}) as well as low-molecular organic acids (acetate, propionate, formate and oxalate). The presence of these compounds may be critical as electron donors of acceptors. Samples (10 g) were re-suspended in 20 ml of sterile distilled water, mixed in a vortex and then thoroughly agitated for 1 h. The mineral particles were removed by centrifugation at 2000 *g* for 10 min and the supernatants loaded into a Metrohm 861 Advanced Compact Ion Chromatographer IC (Metrohm AG, Herisau, Switzerland) as described (Parro *et al*., 2011b). Total protein and sugar content in the samples was determined in the field laboratory as described (Parro *et al*., 2011b), and crude whole extracts were prepared from 20 to 40 g of different samples with 1× PBS (Phosphate Buffered Saline), 0.2 M EDTA as previously reported (Schweitzer *et al*., 2005; Parro *et al*., 2008). See Supporting Information for details.

Antibody production, purification, labeling, and construction of LDChip300

The antibodies used in this study (Table S2) were the result of several years of work aimed at the detection of molecular biomarkers for planetary exploration and environmental monitoring. At the time of the present study we had a collection of 300 antibodies, which constituted the so called immunosensor LDChip300. The criteria for antibody production and selection were explained previously in Parro and colleagues (2005), Parnell and colleagues (2007), Parro and colleagues (2008), Rivas and colleagues (2008), and Parro and colleagues (2011b). Antibodies were produced against bacterial strains from the most representative phyla (Parro *et al*., 2011b; Table S2 in Supporting Information), with those of *Gammaproteobacteria* being the most numerous. Particularly relevant for this work, was the presence of 24 antibodies (from IVF1 . . . to IVF7 . . . in Table S2) from different extracts and culture conditions of five psychrophile bacterial strains: *S. gelidimarina*, *P. burtonensis*, *Psychrobacter frigidicola*, *Cr. psychrophilum*, and *C. psychrerythraea.* Additionally, antibodies to three methanogenic Archaeal strains were also included: the psychrophile *Methanococcoides burtonii*, and the mesophiles *Methanobacterium formicicum* and *Methanosarcina mazeii.* All the antibodies were purified by Protein A affinity purification and fluorescently labelled as reported previously in Parro and colleagues (2005) and Rivas and colleagues (2008).

The LDChip300 antibody microarrays were constructed as described by Parro and colleagues (2011b). Briefly, (i) we used a commercial protein printing buffer 2× (Whatman, Schleicher & Schuell, Sandford, ME) and 0.02% Tween 20 as the spotting solution and (ii) printing was done in a duplicate spot-pattern on epoxy-activated glass slides (Arrayit Corp., Sunnyvale, CA) with a MicroGrid II TAS arrayer (Biorobotics, Genomic Solutions, UK). Up to nine different arrays containing a duplicate spot pattern for the 300 antibodies were spotted on a microscope slide so that each microarray (LDChip300) fits with one of the nine flow cells in a multi-array analysis module device (Parro, 2010; Parro *et al*., 2011b).

Sample processing and sandwich microarray immunoassay procedure

Different core samples were collected, fractionated in the base laboratory, and analysed by SMI with LDChip 300. Up to 0.5 g of core samples were sonicated in 1 ml of TBSTRR buffer (0.4 M Tris-HCl pH 8, 0.3 M NaCl, 0.1% Tween 20) with a manual sonicator for 3 × 1 min cycles (DR. HIELSCHER 50W DRH-UP50H sonicator, Hielscher Ultrasonics, Berlin, Germany). The sonicated samples were filtered through 20 μm nylon filters to remove sand and coarse material. Then, 50 μl of the filtrate were inoculated into one of the nine flow cells of the multi-array analysis module device to flood the LDChip300. After 1 h of incubation at ambient temperature, the flow cells were washed with TBSTRR and the immunoassay revealed by 1 h incubation with a mixture of 300 different fluorescent antibodies, as described elsewhere (Parro *et al*., 2011b). Superficial pyroclasts were ground with a mortar and pestle, extracted by sonication, filtered and incubated with LDChip300 as indicated above.

Optical and scanning electron microscopy and viable cell counting

Samples were analysed by FISH as described by Amann and colleagues (1995) and Lunau and colleagues (2005) with some modifications. Briefly, samples (5–6 g) were added to 25 ml of 1× PBS and 285 μl of 10% (v/v) of sterile methanol and subjected to mild sonication (50/60 Hz at ambient temperature for 15 min) to detach microorganisms from soil. Afterwards the sample was centrifuged at 2000 *g* for 1 min and the supernatant was recovered. Two different fixation protocols were carried out: (i) with paraformaldehyde (PFA), recommended for Gram-negative prokaryotes, and (ii) with ethanol (EtOH), recommended for gram-positives. For the former, 3 vols of 4% PFA: 1× PBS (3:1) were added to 1 vol of supernatant (see above) and incubated for 2 h at 4°C. The fixed sample was then centrifuged for 2 min at 5000 *g* and the fixative (supernatant) was removed. The sample was then washed three times with 1× PBS, with centrifugation at 12 000 *g* for 3 min between washes, and stored in 1× PBS : ethanol (1:1) at –20°C until further processing. For Ethanol fixation, 1 vol of ice-cold 96–100% EtOH (molecular grade) was added to 1 vol of cell containing supernatant and it was stored at –20°C until further processing. For FISH studies, 40 μl of PFA fixed sample (20 μl × 2 times) and 40 μl of EtOH fixed sample (20 μl × 2 times) were dropped onto a well of a glass slide. After each addition of PFA or EtOH, the slides were dried at room temperature, and then they were immersed in 50%, 80% and 96% ethanol for 3 min each. Cy3- and Fluorescein-labelled oligonucleotide probes at the 5′ end were purchased from Fisher Scientific (Waltham, Massachusetts, USA). Samples

were incubated in 18 μl of the hybridization buffer [0.9 M NaCl, 20 mM Tris-HCl, 0.01% sodium dodecyl sulphate (SDS)] in the presence of 5.5 ng ml^{-1} of each labeled probe (Fluorescein-ARC 915 for archaea and Cy3-EUB338a for most eubacteria) and the probe-specific formamide concentration (20% for ARC 915 and 35% for EU338a) at 46°C for 2 h. After hybridization, the slides were washed for 15 min at 48°C in 50 ml of buffer solution containing 20 mM Tris-HCl, 5 mM EDTA, 0.01% SDS and either 225 or 80 mM NaCl depending on the formamide concentration during hybridization (20% and 35% respectively), subsequently rinsed with distilled water and air-dried. Samples were stained with DAPI (1 mg ml^{-1}) for 3 min and further washed with distilled water. To remove unspecific DAPI binding the slides were immersed in absolute ethanol to avoid background fluorescence. A small drop of Vecta Shield solution (Vector Laboratories, CA) was added and preparations were stored at –20°C until visualization.

Scanning electron micrographs were made with gold-coated pieces of core samples with a JEOL JSM-5600 LV instrument (JEOL, Tokyo, Japan). To examine the micromorphology and mineralogy, it was operated at acceleration voltages of 10–20 kV and 2–3 kV. The elemental compositions were measured with energy-dispersive X-ray (EDX, INCA X-Sight, Oxford), with acceleration voltages of 10 kV for minerals and 2 kV for microorganisms. For viable cell counting, the supernatants obtained after minerals removal (see *Geochemical analysis*), were immediately spread onto LB plates and incubated at 20°C for up to 9 days for colonies counting.

DNA extraction, microarray hybridization and phylogenetic analysis

Environmental DNA was extracted from 2 g of sample with the Ultraclean Soil DNA kit (MoBio laboratories, Inc.). This DNA was used as template for PCR amplification with the bacterial universal primers 16SF as forward (positions 8–27 of *Escherichia coli* 16S rRNA, 5′-AGAGTTTAGTCATGGCTCA) and 16SR as reverse one (positions 1057–1074, 5′-CACGAGCTGACGACAGCCG) for16S rRNA gene; and 23SF (positions 105–127; 5′ GCGATTTCYGAAYGGGGRAACCC) and 2241R (positions 2236–2253; 5′ ACCGCCCCAGTHAAACT) for *E. coli* 23S rRNA gene. For PCR amplification the thermocycler was programmed as follows: 95°C 5 min; 30X (95°C 20 s, 56°C 30 s, 72°C 2 min); 72°C 10 min; 4°C. The PCR products were purified with Qiagen PCR purification kit columns.

For microarray hybridization we used the prokaryotic acidophile microarray, an oligonucleotide microarray containing specific probes for prokaryotic microorganisms, printed and treated as described by Garrido and colleagues (2008). Although this microarray was initially developed for the detection of prokaryotic acidophiles, it also contains specific oligonucleotide probes for the 16S and 23S rRNA genes from other universal groups: *Alpha*-, *Beta*-, *Gamma*- and *Deltaproteobacteria*, *Firmicutes* (low-GC-content), high-GC-content Gram-positive bacteria, Archaea, etc. See Supporting Information for details.

For sequencing, the extracted environmental DNA was used as template for PCR amplification of the bacterial 16S rRNA gene with the primer pair 16SF-16SR. The products from this reaction were cloned, sequenced, and analysed as described previously (Parro *et al*., 2011b).

Acknowledgements

We thank Marina Postigo for technical assistance and the personnel of the Spanish BAE 'Gabriel de Castilla', headed by Commandant José Gonzálvez, for their help in the field. This work has been funded by the Spanish Ministerio de Ciencia e Innovación, Subdirección de Política Científica, granted project AYA2008-04013.

References

Amann, R.I., Ludwig, W., and Schleifer, K.H. (1995) Phylogenetic identification and in situ detection of individual microbial cells without cultivation. *Microbiol Mol Biol Rev* **59:** 143–169.

Andrews, S.C., Robinson, A.K., and Rodríguez-Quiñones, F. (2003) Bacterial iron homeostasis. *FEMS Microbiol Rev* **27:** 215–237.

Baker, P.E., and McReath, I. (1971) 1970 volcanic eruption at Deception island. *Nat Phys Sci* **231:** 5–9.

Bowman, J.P., McCammon, S.A., Brown, J.L., Nichols, P.D., and McMeekin, T.A. (1997a) *Psychroserpens burtonensis* gen. nov., sp. nov., and *Gelidibacter algens* gen. nov., sp. nov., psychrophilic bacteria isolated from Antarctic lacustrine and sea ice habitats. *Int J Syst Bacteriol* **47:** 670–677.

Bowman, J.P., McCammon, S.A., Nichols, D.S., Skerratt, J.H., Rea, S.M., Nichols, P.D., and McMeekin, T.A. (1997b) *Shewanella gelidimarina* sp. nov. and *Shewanella frigidimarina* sp. nov., novel Antarctic species with the ability to produce eicosapentaenoic acid (20:5 omega 3) and grow anaerobically by dissimilatory Fe(III) reduction. *Int J Syst Bacteriol* **47:** 1040–1047.

Cameron, R.E., and Benoit, R.E. (1970) Microbial and ecological investigations of recent cinder cones. Deception Island. Antarctica-a preliminary report. *Ecology* **51:** 802–809.

Garrido, P., González-Toril, E., García-Moyano, A., Moreno-Paz, M., Amils, R., and Parro, V. (2008) An oligonucleotide prokaryotic acidophile microarray (PAM): its validation and its use to monitor seasonal variations in extreme acidophilic environments with total environmental RNA. *Environ Microbiol* **10:** 836–850.

Gilichinsky, D.A., Wilson, G.S., Friedmann, E.I., McKay, C.P., Sletten, R.S., Rivkina, E.M., *et al.* (2007) Microbial populations in Antarctic permafrost: biodiversity, state, age, and implication for astrobiology. *Astrobiology* **7:** 275–311.

Hallberg, K.B., Hedrich, S., and Johnson, D.B. (2011) *Acidiferrobacter thiooxydans*, gen. nov. sp. nov.; an acidophilic, thermo-tolerant, facultatively anaerobic iron- and sulfur-oxidizer of the family Ectothiorhodospiraceae. *Extremophiles* **15:** 271–279.

Hirsch, P., Gallikowski, C.A., Siebert, J., Peissl, K., Kroppenstedt, R., Schumann, P., *et al.* (2004) *Deinococcus frigens* sp. nov., *Deinococcus saxicola* sp. nov., and *Deinococcus marmoris* sp. nov., low temperature and draught-tolerating, UV-resistant bacteria from continental Antarctica. *Syst Appl Microbiol* **27:** 636–645.

Ishii, S., Yamamoto, M., Kikuchi, M., Oshima, K., Hattori, M., Otsuka, S., and Senoo, K. (2009) Microbial populations responsive to denitrification-inducing conditions in rice paddy soil, as revealed by comparative 16S rRNA gene analysis. *Appl Environ Microbiol* **75:** 7070–7078.

Knoblauch, C., Sahm, K., and Jørgensen, B.B. (1999) Psychrophilic sulfate-reducing bacteria isolated from permanently cold arctic marine sediments: description of *Desulfofrigus oceanense* gen. nov., sp. nov., *Desulfofrigus fragile* sp. nov., *Desulfofaba gelida* gen. nov., sp. nov., *Desulfotalea psychrophila* gen. nov., sp. nov. and *Desulfotalea arctica* sp. nov. *Int J Syst Bacteriol* **49:** 1631–1643.

Lin, B., Hyacinthe, C., Bonneville, S., Braster, M., Van Cappellen, P., and Röling, W.F. (2007) Phylogenetic and physiological diversity of dissimilatory ferric iron reducers in sediments of the polluted Scheldt estuary, Northwest Europe. *Environ Microbiol* **9:** 1956–1968.

Lunau, M., Lemke, A., Walther, K., Martens-Habbena, W., and Simon, M. (2005) An improved method for counting bacteria from sediments and turbid environments by epifluorescence microscopy. *Environ Microbiol* **7:** 961–968.

Marx, J.G., Carpenter, S.D., and Deming, J.W. (2009) Production of cryoprotectant extracellular polysaccharide substances (EPS) by the marine psychrophilic bacterium *Colwellia psychrerythraea* strain 34H under extreme conditions. *Can J Microbiol* **55:** 63–72.

Parnell, J., Cullen, D., Sims, M.R., Bowden, S., Cockell, C.S., Court, R., *et al.* (2007) Searching for life on Mars: selection of molecular targets for ESA's aurora ExoMars mission. *Astrobiology* **7:** 578–604.

Parro, V. (2010) Antibody microarrays for environmental monitoring. In *Handbook of Hydrocarbon and Lipid Microbiology*. Timmis, K.N. (ed.). Berlin, Germany: Springer-Verlag, pp. 2699–2710.

Parro, V., Rodríguez-Manfredi, J.A., Briones, C., Compostizo, C., Herrero, P.L., Vez, E., *et al*. (2005) Instrument development to search for biomarkers on mars: terrestrial acidophile iron-powered chemolithoautotrophic communities as model systems. *Planet Space Sci* **53:** 729–737.

Parro, V., Fernández-Calvo, P., Rodríguez Manfredi, J.A., Moreno-Paz, M., Rivas, L.A., García-Villadangos, M., *et al*. (2008) SOLID2: an antibody array-based life-detector instrument in a Mars Drilling Simulation Experiment (MARTE). *Astrobiology* **8:** 987–999.

Parro, V., de Diego-Castilla, G., Rodríguez-Manfredi, J.A., Rivas, L.A., Blanco-López, Y., Sebastián, E., *et al*. (2011a) SOLID3 a multiplex antibody microarray-based optical sensor instrument for in situ life detection in planetary exploration. *Astrobiology* **11:** 15–28.

Parro, V., de Diego-Castilla, G., Moreno-Paz, M., Blanco, Y., Cruz-Gil, P., Rodríguez-Manfredi, J.A., *et al*. (2011b) A microbial oasis in the hypersaline Atacama subsurface discovered by a life detector chip: implications for the search of life on Mars. *Astrobiology* **11:** 969–996.

Parro, V., Fernández-Remolar, D., Rodríguez-Manfredi, J.A., Cruz-Gil, P., Rivas, L.A., and Ruiz-Bermejo, M. (2011c) Classification of modern and old río tinto sedimentary deposits through the biomolecular record using a life marker biochip: implications for detecting life on mars. *Astrobiology* **11:** 29–44.

Rabus, R., Ruepp, A., Frickey, T., Rattei, T., Fartmann, B., Stark, M., *et al*. (2004) The genome of *Desulfotalea psychrophila*, a sulfate-reducing bacterium from permanently cold Arctic sediments. *Environ Microbiol* **6:** 887–902.

Rivas, L.A., García-Villadangos, M., Moreno-Paz, M., Cruz-Gil, P., Gómez-Elvira, J., and Parro, V. (2008) A 200-antibody microarray biochip for environmental monitoring: searching for universal microbial biomarkers through immunoprofiling. *Anal Chem* **80:** 7970–7979.

Rivas, L.A., Aguirre, J., Blanco, Y., González-Toril, E., and Parro, V. (2011) Graph-based deconvolution analysis of multiplex sandwich microarray immunoassays: applications for environmental monitoring. *Environ Microbiol* **13:** 1421–1432.

Sattley, W.M., and Madigan, M.T. (2006) Isolation, characterization, and ecology of cold-active, chemolithotrophic, sulfur-oxidizing bacteria from perennially ice-covered Lake Fryxell, Antarctica. *Appl Environ Microbiol* **72:** 5562–5568.

Schweitzer, M.H., Wittmeyer, J., Avci, R., and Pincus, S. (2005) Experimental support for an immunological approach to the search for life on other planets. *Astrobiology* **5:** 30–47.

Selenska-Pobell, S. (2002) Diversity and activity of bacteria in uranium mining waste piles. In *Radioactivity in the Environment: Interaction of Microorganisms with Radionuclides*. Vol. 22. Keith-Roach, M.J., and Lievens, F.R. (eds). Oxford, UK: Elsevier, pp. 225–254.

Sikorski, J., Tindall, B.J., Lowry, S., Lucas, S., Nolan, M., Copeland, A., *et al*. (2010) Complete genome sequence of *Meiothermus silvanus* type strain (VI-R2). *Stand Genomic* Sci **3:** 37–46.

Sizova, M., and Panikov, N. (2007) *Polaromonas hydrogenivorans* sp. nov., a psychrotolerant hydrogen-oxidizing bacterium from Alaskan soil. *Int J Syst Evol Microbiol* **57:** 616–619.

Smith, P.H., Tamppari, L.K., Arvidson, R.E., Bass, D., Blaney, D., Boynton, W.V., *et al*. (2009) H2O at the Phoenix landing site. *Science* **325:** 58–61.

Stanley, S.O., and Rose, A.H. (1967) Bacteria and yeasts from lakes on Deception Island. *Philos Trans R Soc Lond B Biol Sci* **252:** 199–207.

Steven, B., Leveille, R., Pollard, W.H., and Whyte, L.G. (2006) Microbial ecology and biodiversity in permafrost. *Extremophiles* **10:** 259–267.

Steven, B., Niederberger, T.D., and Whyte, L.G. (2009) Bacterial and archaeal diversity in permafrost. In *Permafrost Soils*. Margesin, R. (ed.). Berlin, Germany: Springer-Verlag, pp. 59–72.

Suzuki, K., Sasaki, J., Uramoto, M., Nakase, T., and Komagata, K. (1997) *Cryobacterium psychrophilum* gen. nov., sp. nov., nom. rev., comb. nov., an obligately psychrophilic actinomycete to accommodate '*Curtobacterium psychrophilum*' Inoue and Komagata 1976. *Int J Syst Bacteriol* **47:** 474–478.

Wagner, D. (2008) Microbial communities and processes in Arctic permafrost environments. In *Microbiology of Extreme Soils*. Dion, P., and Nautiyal, C.S. (eds). Berlin, Germany: Springer-Verlag, pp. 133–154.

Williams, P.J., and Smith, M.W. (1989) *The Frozen Earth: Fundamentals of Geocryobiology*. Cambridge, UK: Cambridge University Press.

Yergeau, E., Hogues, H., Whyte, L.G., and Greer, C.W. (2010) The functional potential of high Arctic permafrost revealed by metagenomic sequencing, qPCR and microarray analyses. *ISME J* **4:** 1206–1214.

Supporting information

Additional Supporting Information may be found in the online version of this article:

Fig. S1. Phylogenetic tree from the 16S rRNA gene sequence of the prokaryotic species to which we have produced antibodies and are represented in LDChip300.
Fig. S2. Sandwich microarray immunoassay analysis of the whole geo-biochemical extracts (with PBS-EDTA) with LDChip300. Several permafrost samples were extracted with PBS-EDTA buffer as indicated in Experimental procedures and then analysed with LDChip300 by sandwich microarray immunoassay. The images on the left show two positive reactions (IVE4C1, C2) corresponding to different antibodies against *Acidithiobacillus thiooxidans* cells (left panel) and the corresponding negative control (right panel). The charts (right) correspond to all the immunograms obtained for the different samples (***0***, ***60***, ***201***, etc) with LDChip300. Fluorescent intensity scale ranges from 0 to 30 000 relative units. Peaks numbers correspond to antibodies: 1, IA2S1; 2, IA3S1; 3, IC1C1; 4, IC2C3; 5, IC3S2; 6, IC4C1; 7, ID1S1; 8, 253; 9, IVE1S1; 10, IVE3S1; 11, IVE3S100; 12, IVE5S100; 13, IVF4S2; 14, IVI5S1 (*Shewanella oneidensis*, anaerobic growth in fumarate); 15, IVJ1C1 (*Haloferax mediterranii*); 16, IVJ8C1 (*Halorubrum* sp.); 17, FeReTs_983; 18, HscA2_1487; 19, ModA2_1494; 20, NifD2_1485; 21, AMP; 22, Dinitrofenol; 23, Humic acids; 24, Naphthalene; 25, Trp; 26, IVE4C1; 27, IVE4C2; 28, IVE4S100; 29, A185; 30, A1496 (see Table S2 for description).
Fig. S3. Viable aerobic cell counting in the Deception Island permafrost. A–E show the morphology after 9 days of incubation at 20°C of the colonies obtained from samples at different depths: A, ***30***; B, ***51***, C, ***90***; D, ***111***; E, ***250***. (Right) DAPI staining of the corresponding colonies (numbers) on the plates.
Fig. S4. Detection of prokaryotes in the Deception Island permafrost with prokaryotic acidophile microarray oligonucleotide microarray containing16S and 23S rRNA gene oligonucleotide probes for different phylogenetic groups of prokaryotes (Garrido *et al*., 2008). (Top) Scanned images obtained after hybridization of PCR amplified and fluorescently labeled environmental 16S and 23S rRNA genes from different depths (samples ***0***, ***60***, ***70***, ***300***, ***340***, ***415***) with prokaryotic acidophile microarray. Positive signals obtained with 16S rRNA gene (green rectangles) and with 23S rRNA one (red) are highlighted. (Bottom) Charts obtained after quantification of the fluorescent signals from the images. Probes showing most relevant positive results are indicated: Y2R and EU338, Bacteria; ALF968, *Alphaproteobacteria*; BET42a, *Betaproteobacteria*; GAM42a, *Gammaproteobacteria*; DELTA495a, *Deltaproteobacteria* and *Gemmatimonadetes*; DELTA385, *Deltaproteobacteria*; LGC354a,b,c, Low GC Gram-positive *Firmicutes* group of Bacteria; HGC236 and HGC1901, High GC Gram positive bacteria (mainly *Actinobacteria*); 1Af, Archaea. Green bars for 16S rRNA and red ones for 23S rRNA.
Fig. S5. Bacterial diversity of Deception Island permafrost obtained by 16S rRNA gene sequencing. Rarefaction curves obtained for the different clusters of samples, as a function of the depth intervals (top numbers), at genetic distances of 0, 0.03, 0.05 and 0.1.
Fig. S6. Phylogenetic tree with all OTU representative sequences from the 16S rRNA gene clones obtained from Deception Island permafrost. The tree contains representative 16S rRNA gene sequences from 117 OTUs defined at a genetic distance of 0.03, together with their best matching type strain and environmental sample sequences. The sequence of *Sulfolobus acidocaldaricus* was included as an out-group. OTU representative sequences are represented by an alphanumeric identifier, in bold type; numbers enclosed in square brackets indicate the number of sequences included in each OTU. Reference sequences are represented by accession number and name or condensed description. Branch labels correspond to bootstrap values. Main taxonomic groups are indicated on the right.
Table S1. List of the permafrost core samples taken in the drill.
Table S2. List of all the antibodies used in this work (also found in Parro *et al*., 2011a).
Table S3. List of the antibodies that showed positive reactions after analysing the surface samples with LDChip300.
Table S4. Viable aerobic cell count Aerobic viable cells as colony forming units per gram of sample along the permafrost column after 9 days at 20°C.
Table S5. List of the sequenced colonies.

Please note: Wiley-Blackwell are not responsible for the content or functionality of any supporting materials supplied by the authors. Any queries (other than missing material) should be directed to the corresponding author for the article.